Functional characterization of I_h-channel splice variants from *Apis mellifera*

Günter Gisselmann*,[1], Christian H. Wetzel[1], Maike Warnstedt, Hanns Hatt

Fakultät für Biologie, Lehrstuhl für Zellphysiologie, ND4, Ruhr-Universität-Bochum, Universitätsstrasse 150, D- 44780 Bochum, Germany

Received 4 June 2004; revised 12 August 2004; accepted 12 August 2004

Available online 7 September 2004

Edited by Maurice Montal

Abstract **We isolated splice variants of the AMIH cDNA by means of polymerase chain reaction and homology screening. Splicing at one site generates at least four different channel transcripts (AMIH, $AMIH_L$, $AMIH_M$ and $AMIH_T$), which code for ion-channel proteins that vary in the interloop regions between the membrane-spanning domains S4 and S5. HEK293 cells in which the $AMIH_L$ splice variants were functionally expressed generated currents that were activated by hyperpolarizing voltage steps. Compared to AMIH, $AMIH_L$ cells showed pronounced differences in the voltage dependency of activation: the incorporation of 32 extra amino acids between S4 and S5 shifts the activation curve by +25 mV. Intracellular cAMP made the current-activation potential still less negative and accelerated the activation more effectively than it does in AMIH cells. In vertebrates, functional diversity of I_h-channels is generated by four different genes. In *Apis mellifera*, splice variants coded by the single gene *AMIH* could generate a similar diversity.**

Keywords: HCN-channel; cAMP; Hyperpolarization- and cyclic nucleotide-activated channel; I_h-channel; Splice variant; *Apis mellifera*

1. Introduction

The hyperpolarization-activated cation current (I_h) is widely distributed in excitable cells. I_h-channels have been shown to play important roles in regulation of cellular excitability, rhythmic activity, and synaptic function. Recently, cDNAs encoding hyperpolarization-activated and cyclic-nucleotide-gated (CNG) cation channels (abbreviated as I_h- or HCN-channels) have been cloned from several invertebrates, including *Drosophila melanogaster*, *Heliothis virescens*, sea urchin, lobster and *Apis mellifera* [1–5]. Channels of this type show sequence homology to both CNG channels [6,7] and voltage-gated potassium channels [8,9] and form a new class within the superfamily of ion channels activated by these factors: recombinantly expressed I_h-channels are dually gated by hyperpolarization and cyclic nucleotides [10]. Such an ion channel is probably composed of four subunits [10], each of which contains six transmembrane segments, a pore region and cytosolic N- and C-termini. The C-terminus of I_h-channels additionally contains a cyclic-nucleotide-binding domain (CNBD) homologous to those of other cyclic-nucleotide-binding proteins, including the (CNG) channels [11]. Unlike most voltage-gated K^+ channels, I_h-channels activate in response to hyperpolarization. Intracellular cAMP, by directly binding to the CNBD, makes these channels responsive to less hyperpolarized potentials, and thus facilitates channel opening [11]. I_h-channels differ in their voltage activation, modulatory action of cyclic nucleotides and activation and inactivation kinetics [7,12]. Some biophysical and pharmacological properties can be assigned to particular regions of the ion channel proteins. For example, Glu_{235} in the S3–S4 linker residue of HCN1 influences activation gating, probably by acting as a surface charge [13]. The S4 segment has been demonstrated to constitute the main component of the voltage sensor in calcium, sodium, and potassium channels [14]. In I_h-channels the S4 domain has a similar role [15–17], so it is likely that the S4–S5 linker, located at the intracellular end of the S4 domain, is the structure mediating communication between the voltage sensor and the activation gate in these types of ion channels [18]. Interactions between S4 and S5 linker and S6 transmembrane domain modulate gating of HERG K^+ channels [19]. This region is significant for I_h-channel gating as well [20], and a molecular coupling of S4–S5 to the C-linker has recently been demonstrated [21].

In contrast to mammals, which have four genes for functionally distinct channel subtypes [7], invertebrates appear to contain only a single I_h-channel gene [2–4]. We were particularly interested in learning whether insects nevertheless also have several functionally different I_h-channels. Our working hypothesis was that a potential variability could be coded by expression of different splice variants of the AMIH mRNA. We have now obtained three splice variants that differ from AMIH in the loop between S4 and S5, called $AMIH_L$, $AMIH_M$ and $AMIH_T$. Here, we present the molecular structure of these variants as well as the results of experiments to detect functional differences, in which the cloned cDNAs were functionally expressed in HEK293 cells and investigated by voltage-clamp measurements.

2. Materials and methods

2.1. RT-PCR

mRNA from heads and bodies of adult *Apis mellifera* workers was isolated by standard methods. cDNA was constructed by using the Moloney murine leukemia virus reverse transcriptase (Invitrogen,

* Corresponding author. Fax: +49-234-32-14129.
E-mail address: guenter.gisselmann@rub.de (G. Gisselmann).

[1] Both authors contributed equally to this work.

0014-5793/$22.00 © 2004 Published by Elsevier B.V. on behalf of the Federation of European Biochemical Societies.
doi:10.1016/j.febslet.2004.08.043

Carlsbad, CA) and oligo(dT_{12-18}) primer. The amino acid sequence from the BCNG-1 channel [22] was used to design PCR primers P1 GAYTTYCGNTTYTAYTGGGA and P2 AGNAGRCANATY-TCNCCRAA derived from amino acids 133–139, 545–551, respectively. The amplification was done for 35 cycles (94° 1 min, 58° 1 min, 72° 1 min, 2.5 units of *Taq*-Polymerase) with 100 pmols of P1 and P2 according to the manufacturer's recommendations (Invitrogen, Carlsbad, CA). PCR products were resolved on a 1% agarose gel.

2.2. cDNA library screen

We screened approximately 2×10^6 plaque-forming units of an *Apis mellifera* head cDNA library in lambda ZAP II with the digoxigenin-labeled 1235 bp PCR product from adult *Apis mellifera* [1]. The hybridization was performed in 5× SSC; 10 ng/μl labeled DNA; 1.0% blocking reagent for nucleic acid hybridization; 0.1% N-lauroylsarcosine; and 0.02% SDS at 65 °C as described in the manufacturer's protocol (Roche, Mannheim, Germany). The final stringency washes were done at 65 °C in 0.1× SSC/0.1% SDS. For detection, nitrocellulose filters were incubated with alkaline phosphatase-labeled antidigoxigenin antibody (Roche, Mannheim, Germany), and positive plaques were visualized by staining with the substrates nitroblue tetrazolium and 5-bromo-4-chloro-3-indolyl phosphate for several hours. 20 positive plaques were randomly chosen, picked, plaque purified and in vitro excised into pBluescript plasmid.

2.3. Construction of expression vectors

In order to construct vectors suitable for expression of AMIH in HEK293 cells, the open reading frame of the AMIH splice variants was amplified by PCR performed with $pAMIH_L$ or $pAMIH_T$ as template, respectively. The amplification was done for 25 cycles (94° 1 min, 60° 1 min, 72° 3 min, 2.5 units of *Taq*-Polymerase, 0.125 unit of *Pfu*-Polymerase) with 30 pmols of P3 (GGCTAAGCTTGCCATGA-ATTACAAGGGCGGGAAG) and P4 (CGTCTAGATCCTGGA-CAACTGG) according to the manufacturer's recommendations (Invitrogen, Carlsbad, CA). The ~2000 bp PCR products were subcloned into pRC/CMV (Invitrogen, Carlsbad, CA) digested with *Hind*III/*Xba*I and blunt ended with Klenow enzyme and were verified by sequencing. The vector $pAMIH_M$ was constructed by a two step PCR based cloning strategy using $AMIH_T$ as a template and contains essentially the $AMIH_T$ insert lacking exon 9. In the resulting expression vectors, $pAMIH_L$, $pAMIH_M$ or $pAMIH_T$, the corresponding cDNA is under control of a strong CMV-promoter.

2.4. Cell culture and transfection of HEK293 cells

HEK293 cells were grown in minimum essential medium supplemented with 10% fetal calf serum in 5% CO_2 at 37 °C. Transfection was accomplished by mixing 15 μg of expression vector (11 μg $pAMIH_{L,M}$ or $pAMIH_T$ and 4 μg pIRES-EGFP) and 25 μl of 250 mM $CaCl_2$ as described previously [23]. For co-expression experiments, a mixture of 1 μg $pAMIH_L$, 10 μg $pAMIH_T$ and 4 μg pIRES-EGFP or 1 μg $pAMIH_L$, 10 μg pBluescriptKS and 4 μg pIRES-EGFP was used, respectively. pBluescriptKS served as inert carrier DNA to keep the total amount for plasmid DNA used for transfection constant. The material was added dropwise to 250 μl 2× HEPES buffered saline. The precipitate was then added to 20% confluent HEK293 cells and allowed to incubate for 5 h before the cells were washed twice with phosphate buffered saline (137 mM NaCl, 8.1 mM Na_2HPO_4, 2.7 mM KCl, 1.5 mM KH_2PO_4, 0.9 mM $CaCl_2$, and 0.5 mM $MgCl_2$, pH 7.2). Efficiency of transfection, typically 20–40%, was checked by GFP-fluorescence detection of the GFP coded by the pIRES-EGFP plasmid (Clontech, Palo Alto, CA). Measurements were done 24–72 h post transfection.

2.5. Electrophysiology and solutions

Transfected HEK293 cells transiently expressing green fluorescent protein (GFP) and the recombinant AMIH channel were recorded in the whole-cell voltage-clamp configuration [24] under visual control using an inverted microscope (Zeiss, Jena, Germany). The cells were kept in an external solution containing: 138 mM NaCl, 5 mM KCl, 0.5 mM $CaCl_2$, 1.5 mM $MgCl_2$, 10 mM glucose and 10 mM HEPES. pH was adjusted to 7.4 with NaOH. Patch electrodes were pulled from borosilicate glass (Clark Electromedical Instruments, Pangbourne, England) using a horizontal pipette puller (DMZ Universal Puller, Zeitz-Instruments, Munich, Germany) to yield pipettes with resistances of 3–6 MΩ. Pipettes were filled with a solution containing: 140 mM KCl, 0.1 mM $CaCl_2$, 1 mM $MgCl_2$, 5 mM EGTA, 10 mM HEPES, and 2 mM ATP adjusted to 7.3 with KOH. For some experiments, cAMP or cGMP at the concentration indicated was included. After establishing the whole-cell configuration, the series resistance was estimated and checked during the course of the experiment using an EPC-9 amplifier (HEKA instruments, Darmstadt, Germany). The series resistance (typically 10–20 MΩ) and the capacitance were compensated. Depending on the experiment, the recording was done while the cells were attached to the culture dish or after they had been lifted from the substrate. Voltage protocols were delivered and current signals were recorded with an EPC-9 amplifier using the Pulse software on a Macintosh Centris 650 computer. The data were analyzed using the PulseFit (exponential fits of kinetics, HEKA instruments, Darmstadt, Germany), SigmaPlot 8.0 (Student's *t* test, Boltzmann fits, SPSS, Inc) and IgorPro (Wavemetrics, Lake Oswego, Oregon, USA) software. All data are ±S.E.M.

3. Results

3.1. Cloning of cDNA for splice variants of Apis mellifera I_h-channels

To isolate possible splice variants of the AMIH cDNA [1], we screened an *Apis mellifera* head cDNA library and isolated 15 cDNA clones containing inserts with AMIH cDNA. Sequencing revealed that they represented three different populations of splice variants of the AMIH transcript. The sequence in seven of these inserts matched the sequence originally found for the AMIH open reading frame [1]. Five of the remaining eight clones clearly represented splice variants with an additional sequence of 96 nt inserted in the coding region for the interloop region between S4 and S5, coding for 32 additional amino acids. The corresponding cDNA was named $AMIH_L$ (long) (Fig. 1A). The predicted $AMIH_L$ polypeptide consisted of 664 amino acids with a calculated molecular mass of 76.3 kDa. Three of the fifteen isolated clones were found to be splice variants with an additional sequence of 178 nt inserted in the coding region for the interloop region between S4 and S5, coding for 52 additional amino acids, followed by a stop codon; this insert thus codes for a protein with a truncated C-terminal end (Fig. 1). The corresponding cDNA was named $AMIH_T$ (truncated). Analysis of RT-PCR fragments encompassing this region (Fig. 2B) suggests that at least one further splice variant – $AMIH_M$ – is existing. In this variant, 25 amino acids located between S4 and S5 were coded by an additional exon (Figs. 1B and 2A), but so far we were not able to isolate a corresponding full length cDNA out of the *Apis mellifera* cDNA library for this variant.

We addressed the question whether the variants of the AMIH channel protein are located in regions where other I_h-channels are also varying. A comparison of the S4–S5 interloop region with the protein sequences of other I_h-channels revealed that these regions are far less conserved than the rest of the (highly conserved) hydrophobic core region. In this region other I_h-channels show sequence variations and length polymorphisms (Fig. 1B) and in $AMIH_L$ a large cluster of charged amino acids with a positive net charge of about 7 is found there. An analysis of the current genome sequencing data available for *Apis mellifera* in the genebank revealed that the AMIH-mRNA is composed of 14 exons (1–7 and 11–19 in Fig. 2A). The $AMIH_L$ variant possessed an additional exon (10 in Fig. 2A) that coded for the 32 additional amino acids present in this variant. In $AMIH_T$, the two additional exons 8 and 9 are present (Fig. 2A). In $AMIH_M$, 25 amino acids lo-

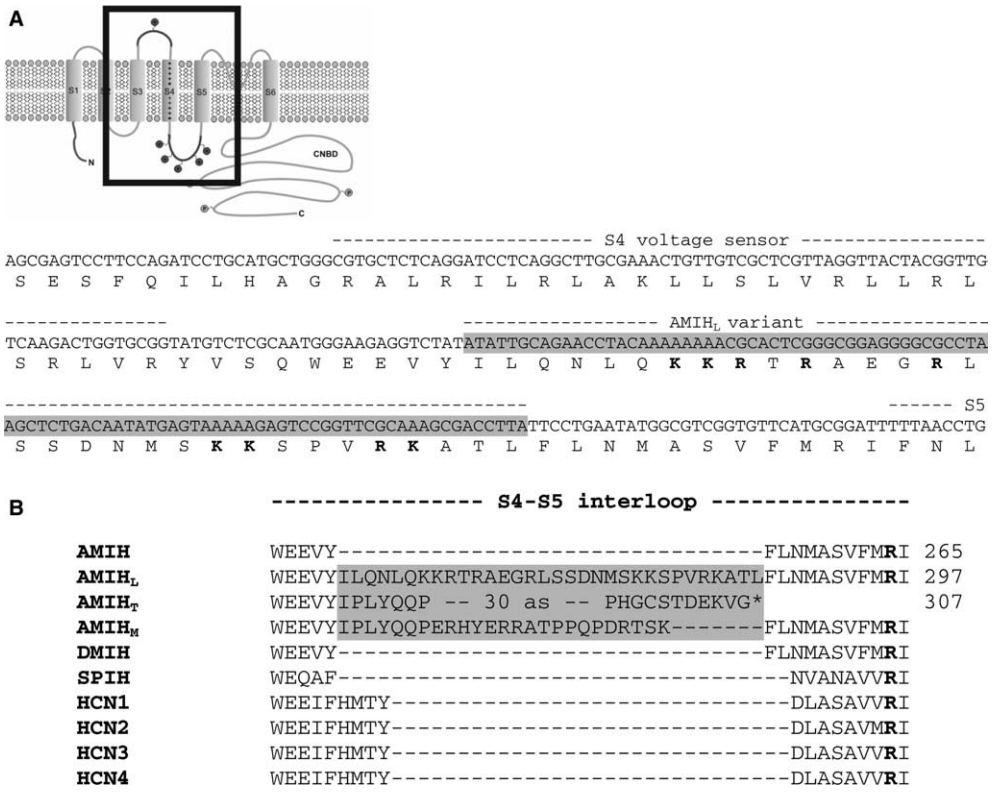

Fig. 1. Sequence of AMIH splice variants. (A) Location of the variants in the interloop regions. The location of the variants is indicated by gray shading. Polar amino acids referred to in the text are indicated by bold type. (B) Comparison of the S4–S5 interloop region of AMIH$_L$, AMIH$_M$ and AMIH$_T$ with AMIH (AY280848), DMIH (NP_610949), SPIH (CAA76493) and HCN1–4 (O88704, O88703, Q9P1Z3 and O70507).

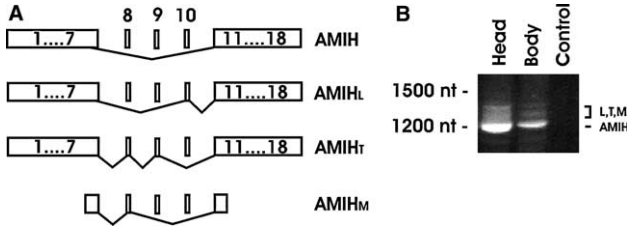

Fig. 2. (A) Location of the exons 8–10 of the *AMIH* gene additionally present in the different splice variants. (B) RT-PCR analysis of AMIH transcripts in *Apis mellifera*. PCR products of 1200 bp length employing P1 and P2 correspond to the variant AMIH, the less abundant larger fragments to the variants AMIH$_{T, M, L}$. No PCR product was amplified in the water control.

cated between S4 and S5 were coded by the additional exon 8 (Figs. 1B and 2A).

3.2. Electrophysiological characterization of heterologously expressed AMIH$_L$

The function of AMIH-channels was analyzed by whole-cell voltage-clamp recording from HEK293 cells transfected with the expression vectors pAMIH$_L$, pAMIH$_M$ or pAMIH$_T$. In cells transfected with AMIH$_L$, hyperpolarizing steps from a holding potential of 0 mV to more negative values (−150 to −30 mV) produced slowly activating inward currents (Fig. 3A), which were never observed in untransfected HEK293 cells or those transfected with pAMIH$_T$ or pAMIH$_M$ (data not shown).

To obtain the instantaneous current–voltage (I/V_m) relationship, cells were hyperpolarized to −150 mV and subsequently stepped to various holding potentials (Fig. 3B). The I/V_m relationship determined from the amplitude of the tail currents (Fig. 3B) was linear in the range from −60 to +40 mV (Fig. 3C). The mean reversal potential, V_{rev}, was -35 ± 8 mV ($n = 13$) under nearly physiological ionic conditions. Using this reversal potential and the concentration of sodium and potassium ions in the Ringer's and pipette solutions, the relative permeability ratio for sodium vs. potassium ions was estimated to be 0.22 for AMIH$_L$, in good agreement with the ratio of 0.24 determined for AMIH [1]. Following activation of the inward currents by hyperpolarizing voltage steps, depolarization of the membrane potential produced a delayed closing of channels. The tail current peak amplitudes showed a sigmoidal dependence on the potential of the activating voltage step (Fig. 4A). The membrane potential for half-maximal activation ($V_{1/2}$) fitted to the Boltzmann equation was -88 ± 2 mV ($n = 7$) with a slope factor of 12.7 mV. With a shift of 25 mV, this $V_{1/2}$ is considerably more positive than the $V_{1/2}$ of -113 ± 5 previously found for AMIH [1]. 1 mM cAMP shifted the activation curve about 29 mV in the positive direction to -59 ± 3 mV ($n = 4$) and decreased the slope factor to 9.5 mV. The time course of activation was strongly dependent on the size of the hyperpolarizing voltage steps. The activation kinetics could be fit by a single exponential function. Tau-values for AMIH$_L$ depended on the membrane potential, ranging from 298 ± 22 ms (at −150 mV) to 1242 ± 104 ms (at −110 mV) (Fig. 4B). These tau values were comparable to those obtained with the previously described splice variant AMIH (Fig. 4B).

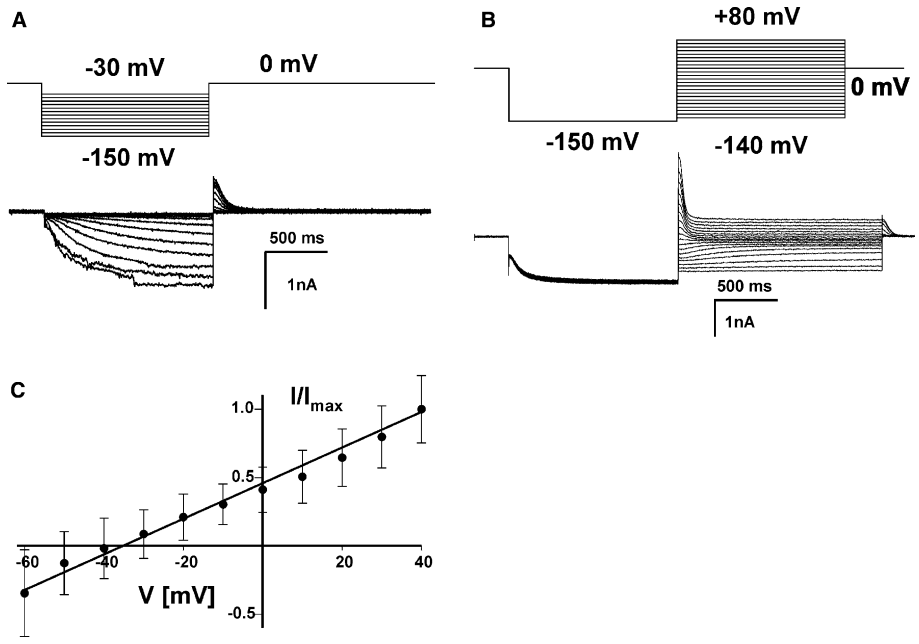

Fig. 3. Functional properties of I_h-currents generated by $AMIH_L$ cells. (A) Currents generated in response to hyperpolarizing voltage steps in HEK293 cells expressing $AMIH_L$. Currents were activated by stepwise hyperpolarization of the membrane potential (for 1200 ms). Membrane potential was set to 0 mV and stepped from −30 to −150 mV in 10 mV increments. Tail currents were induced by stepping the test voltage to 0 mV. (B) Tail currents generated in response to depolarizing voltage steps in HEK293 cells expressing $AMIH_L$. Currents were activated by a voltage step from 0 to −150 mV. Tail currents were recorded at potentials ranging from +80 to −140 mV (10 mV increments). (C) I/V relationship of the tail currents in $AMIH_L$ cells, obtained from tail-current amplitudes measured immediately after the voltage step to the indicated test voltage. The currents reversed at −35 mV. The relative permeability ratio for Na^+ and K^+ (P_{Na}/P_K), as determined by the Goldman–Hodgkin–Katz equation, is 0.22. Currents were activated by the protocol shown in (B).

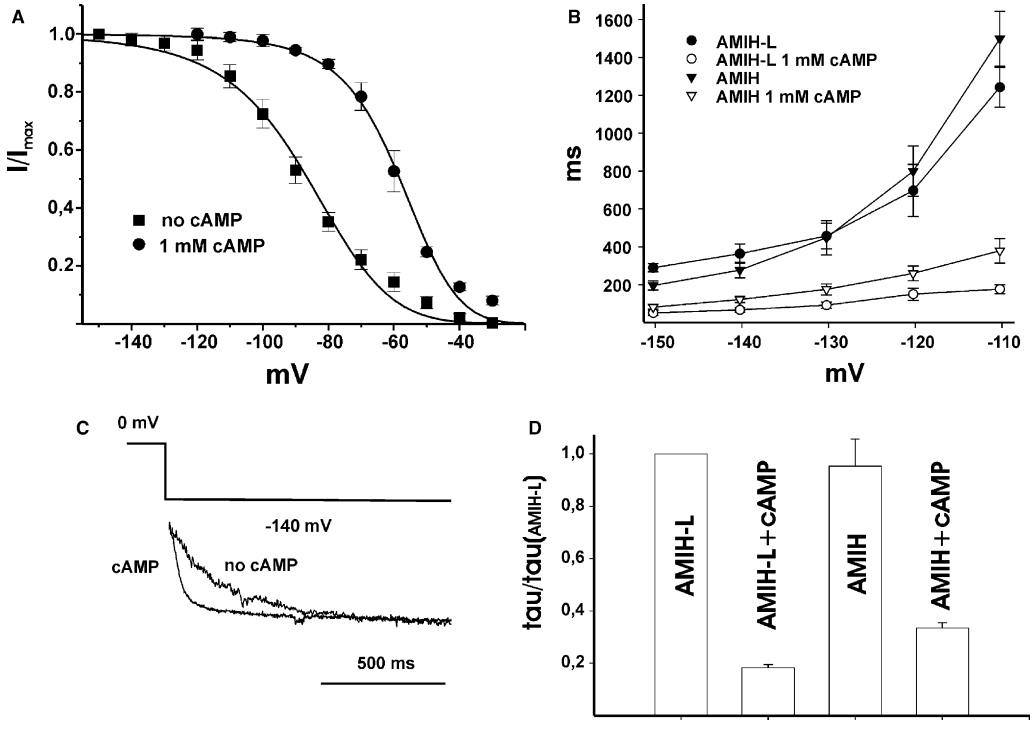

Fig. 4. (A) Voltage dependence of activation and modulation by cAMP (1 mM). Normalized tail-current peak amplitudes measured immediately after the voltage step to 0 mV plotted against membrane potential (protocol shown in Fig. 3A). The data were fitted by the Boltzmann equation. (B) Voltage dependence of the rate of activation. The time constants of AMIH and $AMIH_L$ activation calculated by a monoexponential fit exhibited a strong dependence on membrane potential and were lowered by cAMP (1 mM). Currents were activated by the protocol shown in Fig. 3A. (C) Modulation of the activation kinetics by intracellular cAMP. Currents were activated by hyperpolarizing steps from 0 to −140 mV (1200 ms). 1 mM cAMP in the intracellular solution accelerated the activation kinetics of the channel. (D) Activation kinetics of $AMIH_L$ and AMIH and modulation by intracellular cAMP. The activation kinetics determined in (B) were averaged for each voltage step and normalized to $AMIH_L$ control values.

Cells containing 1 mM cAMP showed a decreased time constant, i.e., an accelerating effect of cAMP on the activation kinetics of inward currents compared to control cells (no cyclic nucleotides in the patch pipette) (Fig. 4C). In the presence of 1 mM cAMP, tau-values decreased to 50 ± 12 ms at −150 mV and 176 ± 23 ms at −110 mV ($n = 5$) (Fig. 4B). To compare the kinetics of AMIH with the $AMIH_L$ splice variants, values were normalized to the $AMIH_L$ tau values and averaged ($n = 25$). AMIH and $AMIH_L$ did not differ significantly in the averaged normalized tau values ($P = 0.67$). In contrast, cAMP decreases the tau values (normalized and averaged in the range of −110 to −150 mV) significantly more in $AMIH_L$ (to 18%) than in AMIH (to 33%) ($P = 0.0002$) (Fig. 4D).

What could be the function of $AMIH_T$? As expected for a truncated ion-channel protein with the pore region missing, $AMIH_T$ does not form functional channels of its own when expressed in HEK293 cells. One possible function could be the downregulation of I_h-channel activity due to a dominant negative effect. In cell-culture systems, it has been shown that the incorporation of mutated subunits can render I_h-channels non-functional. In *Drosophila*, a C-terminal truncated voltage-gated potassium channel interfered with the function of wild type channels in vivo [25]. To test if $AMIH_T$ could serve the same function, we co-expressed it with AMIH. HEK293 cells co-transfected with the expression vectors pAMIH and $pAMIH_T$ in a ratio of 1:10 expressed hyperpolarization-activated channels with comparable amplitudes as cells transfected with the same amount of pAMIH alone ($n = 3$, data not shown). These experiments showed that even an excess of co-transfected $pAMIH_T$ does not interfere in a dominant negative fashion with the AMIH function.

4. Discussion

We isolated splice variants of the AMIH cDNA and found that splicing generated at least four different channel transcripts. These variants code for ion-channel proteins that differ with respect to the intracellular loop between S4 and S5. The AMIH sequence originally isolated from an *Apis* cDNA library [1] is clearly the variant with the shortest loop between S4 and S5.

Expressed in HEK293 cells, the insertion of 32 extra amino acids in the S4–S5 linker of $AMIH_L$ shifted the $V_{1/2}$ in the positive direction, by +25 mV. It is known from investigations of the structure–function relationship that distinct biophysical and pharmacological properties can be assigned to distinct domains of the ion-channel proteins. The AMIH splice variants affected those protein regions in which considerable variation has also been found in the sequence of the distinct mammalian HCN-channel subunits. Therefore, variations in these regions are thought to generate functional diversity. The role of the S4–S5 linkers in HCN- and other ion channels of similar molecular architecture has been investigated in detail. On the basis of its location at the intracellular end of the S4 voltage sensor domain, the S4–S5 linker is a potential candidate for the structural link between the voltage sensor and the activation gate in K_v-, HERG- and HCN-channels [19,21,20,18]. Could the introduced intracellular charges alter the $V_{1/2}$ by a surface charge effect? A more positively charged extracellular S3–S4 linker shifts the $V_{1/2}$ to more positive values [13], therefore, a more positively charged intracellular S4–S5 linker should effect a shift to more negative values, opposite to that shown by the experimental data. For HCN2, it was suggested that interactions between residue R_{339} in the S4–S5 loop and residues D_{443} in the C-linker, a carboxyl-terminus segment that connects S6 to the CNBD, disrupt or stabilize the closed state of HCN2 channels [21] and thus participate in the coupling of voltage sensing and activation gating in HCN channels. The analogous amino acids are conserved in AMIH (R_{246} and D_{350}). It seems possible that the introduction of a large cluster of charged amino acids adjacent to R_{246} alters the possible interaction with the C-linker, thereby shifting the $V_{1/2}$ to more positive values.

The CNBD inhibits hyperpolarization gating in the absence of cAMP. The binding of cAMP shifts gating to more positive values by abolishing this inhibition. The inhibitory effects of the CNBD on gating depend on its interaction with the C-linker and the core transmembrane regions. cAMP binding to the CNBD is likely to cause a conformational change in the C-linker that is coupled to an increased pore opening, ultimately via the N-terminal end of the A′ helix [26,27]. In chimeras between HCN1 and HCN2, it was shown that the interaction of the CNBD with the corresponding C-linker was the major determinant for the maximal $V_{1/2}$ shift caused by cAMP [26,27]. Our results now identify the S4–S5 linker as an additional region that contributes to the modulatory action of cAMP. This is significantly enhanced in $AMIH_L$, which shows a larger $V_{1/2}$ shift and accelerated activation kinetics compared to AMIH. These differences may be caused by a direct interaction of S4–S5 with the CNBD or, indirectly, by a possible interaction of S4–S5 with the C-linker that alters its subsequent interaction with the CNBD. By the investigation of chimeric channels of HCN1 and HCN4, the protein segments S1, S1–S2 and S6-CNBD were identified as crucial regions for the activation gating of HCN channels [28]. Other studies showed that mutations of amino acids S4–S5 can influence the activation kinetics as well [18]. According to our data, however, the insertion of extra amino acids into the S4–S5 loop apparently has no influence on the activation kinetics of AMIH at a given membrane potential.

What are the possible physiological functions of I_h-channels with distinct properties? The $V_{1/2}$ value of I_h-channels influences the oscillatory frequency of neuronal networks in vertebrates and invertebrates [5,10] and the pacemaking activity of the sino-arterial node of the heart [10]. It is possible that in insects differences in I_h-channel properties serve the same function as in other species. An interspecies comparison of $V_{1/2}$ of recombinately expressed invertebrate I_h-channels shows that all variants that possess a short S4–S5 loop – AMIH (−113 mV), *Heliothis* hvCNG (−103 mV) and *Panilirus* PAIH (−119 mV) [1,5,29] – have comparable values. In contrast to that, the variant $AMIH_L$ has a more positive $V_{1/2}$ with −88 mV. Evidence for multiple populations of I_h-channels in the lobster *Panulirus* was given by expression data of *PAIH* RNA injected into pyloric dilator neurons [5]. The *PAIH*-evoked current was different from the endogenous I_h in these neurons: the *PAIH*-encoded current had a more positive $V_{1/2}$ and more rapid activation kinetics [5,30]. Preliminary data have shown that splice variants at similar positions have also been detected in *Panulirus* lobsters (G. Gisselmann, T. Marx, and H. Hatt, unpublished data), what could be a possible explanation for these multiple populations.

What could be the function of $AMIH_T$? As expected for a truncated ion-channel protein with the pore region missing, $AMIH_T$ does not form functional channels of its own when expressed in HEK293 cells. Our data suggest that $AMIH_T$-expression causes no dominant negative effect, although it has to be stated that we could not give the final proof that $AMIH_T$ protein is expressed in a high enough level in our system because the available I_h-channel antibodies detect an epitope not present in the truncated $AMIH_T$-protein. A similar splice variant is found for the *shaker* channel of *Panulirus interruptus* where alternative splicing generates a mRNA lacking the pore forming exon [31]. This mRNA showed also no dominant negative effect when co-expressed with other shaker mRNAs. The putative splice variant $AMIH_M$ possessed an insertion of 25 amino acids between S4 and S5. In contrast to the corresponding insertion of $AMIH_L$ in this interloop, the distribution of charged amino acids differs and the net charge is much lower (+2 vs. +7). We could not achieve any functional expression of this splice variant jet. In future experiment, it has to be shown if it may act as a ß-subunit altering the function of AMIH when co-expressed. In conclusion, we can state that the different splice variants of AMIH may form the molecular basis for the generation of functionally diverse I_h-channels in insects. The AMIH-proteins differ at regions that can in principle serve to modify functional parameters; the results further highlight the importance of the S4–S5 interloop regions for the voltage-sensing and gating properties of I_h-channels.

Acknowledgements: We thank A. Stoeck and H. Bartel for technical assistance, B. Gamerschlag for electrophysiological recordings and A. Bormann for cloning of the splice variants. We are indebted to W. Kirchner for the gift of *Apis mellifera*. This work was supported by the Deutsche Forschungsgemeinschaft GI 255/3 to H.H. and G.G. The Genbank accession numbers for $AMIH_L$ and $AMIH_T$ cDNA sequences are AY739658 and AY739659.

References

[1] Gisselmann, G., Warnstedt, M., Gamerschlag, B., Bormann, A., Marx, T., Neuhaus, E.M., Stoertkuhl, K., Wetzel, C.H. and Hatt, H. (2003) Insect Biochem. Mol. Biol. 33, 1123–1134.
[2] Marx, T., Gisselmann, G., Störtkuhl, K.F., Hovemann, B.T. and Hatt, H. (1999) Invert. Neurosci. 4, 53–63.
[3] Gauss, R., Seifert, R. and Kaupp, U.B. (1998) Nature 393, 583–587.
[4] Krieger, J., Strobel, J., Vogl, A., Hanke, W. and Breer, H. (1999) Insect Biochem. Mol. Biol. 29, 255–267.
[5] Zhang, Y., Oliva, R., Gisselmann, G., Hatt, H., Guckenheimer, J. and Harris-Warrick, R.M. (2003) J. Neurosci. 23, 9059–9067.
[6] Finn, J.T., Grunwald, M.E. and Yau, K.W. (1996) Annu. Rev. Physiol. 58, 395–426.
[7] Santoro, B. and Tibbs, G.R. (1999) Ann. N.Y. Acad. Sci. 868, 741–764.
[8] Pongs, O. (1992) Physiol. Rev. 72, S69–S88.
[9] Catterall, W.A. (1995) Annu. Rev. Biochem. 64, 493–531.
[10] Robinson, R.B. and Siegelbaum, S.A. (2003) Annu. Rev. Physiol. 65, 453–480.
[11] Zagotta, W.N. and Siegelbaum, S.A. (1996) Annu. Rev. Neurosci. 19, 235–263.
[12] Biel, M., Ludwig, A., Zong, X. and Hofmann, F. (1999) Rev. Physiol. Biochem. Pharmacol. 136, 165–181.
[13] Henrikson, C.A., Xue, T., Dong, P., Sang, D., Marban, E. and Li, R.A. (2003) J. Biol. Chem. 278, 13647–13654.
[14] Bezanilla, F. (2000) Physiol. Rev. 80, 555–592.
[15] Bell, D.C., Yao, H., Saenger, R.C., Riley, J.H. and Siegelbaum, S.A. (2004) J. Gen. Physiol. 123, 5–19.
[16] Mannikko, R., Elinder, F. and Larsson, H.P. (2002) Nature 419, 837–841.
[17] Vemana, S., Pandey, S. and Larsson, H.P. (2004) J. Gen. Physiol. 123, 21–32.
[18] Chen, J., Mitcheson, J.S., Tristani-Firouzi, M., Lin, M. and Sanguinetti, M.C. (2001) Proc. Natl. Acad. Sci. USA 98, 11277–11282.
[19] Tristani-Firouzi, M., Chen, J. and Sanguinetti, M.C. (2002) J. Biol. Chem. 277, 18994–19000.
[20] Macri, V.S. and Accili, E.A. (2004) J. Biol. Chem. 279, 16832–16846.
[21] Decher, N., Chen, J. and Sanguinetti, M.C. (2004) J. Biol. Chem. 279, 13859–13865.
[22] Santoro, B., Grant, S.G., Bartsch, D. and Kandel, E.R. (1997) Proc. Natl. Acad. Sci. USA 94, 14815–14820.
[23] Zufall, F., Hatt, H. and Firestein, S. (1993) Proc. Natl. Acad. Sci. USA 90, 9335–9339.
[24] Hamill, O.P., Marty, A., Neher, E., Sakmann, B. and Sigworth, F.J. (1981) Pfluegers Arch. 391, 85–100.
[25] Gisselmann, G., Sewing, S., Madsen, B.W., Mallart, A., Angaut Petit, D., Muller Holtkamp, F., Ferrus, A. and Pongs, O. (1989) EMBO J. 8, 2359–2364.
[26] Wang, J., Chen, S. and Siegelbaum, S.A. (2001) J. Gen. Physiol. 118, 237–250.
[27] Wainger, B.J., DeGennaro, M., Santoro, B., Siegelbaum, S.A. and Tibbs, G.R. (2001) Nature 411, 805–810.
[28] Ishii, T.M., Takano, M. and Ohmori, H. (2001) J. Physiol. 537, 93–100.
[29] Heine, M., Ponimaskin, E., Bickmeyer, U. and Richter, D.W. (2002) Pflugers Arch. Eur. J. Physiol. 443, 418–426.
[30] Kiehn, O. and Harris-Warrick, R.M. (1992) J. Neurophysiol. 68, 496–508.
[31] Kim, M., Baro, D.J., Lanning, C.C., Doshi, M., Farnham, J., Moskowitz, H.S., Peck, J.H., Olivera, B.M. and Harris-Warrick, R.M. (1997) J. Neurosci. 17, 8213–8224.